

Packing Volume of Sedimented Microtubules: Regulation and Potential Relationship to an Intracellular Matrix

P. A. BROWN and R. D. BERLIN

Department of Physiology, University of Connecticut Health Center, Farmington, Connecticut 06032

ABSTRACT To determine the contribution of microtubules to a hypothetical intracellular matrix, we have analyzed the space occupied by microtubules *in vitro*. Taxol-stabilized microtubules assembled from purified (three-times-cycled) bovine brain microtubule protein were pelleted by centrifugation under standardized conditions. The specific volume of the pellet, defined as the microliter volume per milligram protein, was 22.4. As suggested by others, this volume was strongly dependent on microtubule-associated proteins (MAPs), as shown by quantitation of the effects of purified MAP supplementation on specific volume. The specific volumes of microtubule pellets stripped of MAPs by high salt or chymotryptic digestion approached the mathematically optimal (least occupied space) and increased 14-fold with the highest MAP concentrations employed. Packing was also dependent on pH. Specific volumes comparable to those of MAP-depleted microtubules were attainable at pH's from 5.5 to 6.0, and specific volumes more than doubled at pH 7.5. MAP content was unaffected by pH.

We present a theoretical analysis that suggests that as microtubules are centrifuged the mixture behaves as a liquid crystal. With packing, the mixture undergoes an isotropic-nematic phase transition in which the microtubules become oriented principally as parallel rods, mimicking their orientation *in vivo*. From the known concentration of microtubules *in vivo*, it can be inferred from our measurements that in some cells a large fraction, perhaps 40–50% of the cytosolic volume, is occupied by microtubules that form a mechanically irreducible space. Further theoretical analysis employing Ogston's formulation of the penetrability of fibrous networks suggests that the space between microtubules (in contrast to the extracellular matrix) imposes little barrier to the diffusion of macromolecules. A microtubule array thus achieves mechanical stability without affecting transport by diffusion. The space can accommodate other fibrous networks that could then affect transport, and, as we show, the space itself may be regulated by MAP content and intracellular pH.

A clear space or halo that surrounds microtubules is frequently observed by electron microscopy (1). This space is usually attributed to a fuzzy coat surrounding the microtubule that is correlated *in vitro* with the presence of high molecular weight microtubule-associated proteins (HMW-MAPs).¹ Thus thin sections through pellets of microtubules prepared in the presence or absence of HMW-MAPs show that there is tighter packing of MAP-free microtubules (2).

The studies reported here were aimed at further quantitative

analysis of the space occupied by microtubules assembled *in vitro*. We found that when microtubules were pelleted by centrifugation, their volume per milligram protein was comparable to that reported for pellets of glycosaminoglycan-collagen mixtures sedimented with similar force. This encouraged us to ask whether microtubules may contribute to an "intracellular matrix" that is analogous to the familiar glycosaminoglycan (GAG)-collagen-based extracellular matrix (3, 4). We will discuss the relationship of our findings to the packing of microtubules in neurons and erythrocytes and the implications of microtubule density for the movement of particles and molecules. Coupled with the known concentrations of intracellular assembled microtubules, our findings

¹ *Abbreviations used in this paper:* GAG, glycosaminoglycan; HMW-MAP, high molecular weight MAP; MAP, microtubule-associated protein.

suggest that in certain cells or subcellular regions, microtubules account for a major fraction of the intracellular volume.

In addition, it is clear that the spacing between microtubules *in vivo* is variable and may become exceedingly small (5, 6). We thus consider how the space occupied by microtubules might be regulated and found that the packing density of microtubules was a sensitive function of their MAP content and of pH.

MATERIALS AND METHODS

Taxol was obtained from the Drug Synthesis and Chemistry Branch of the National Cancer Institute, courtesy of Dr. M. Suffness. The assembly buffer used in all experiments was 20 mM sodium phosphate, 100 mM glutamic acid adjusted to pH 6.75 (PG buffer), 1.5 mM GTP (type IIS; Sigma Chemical Co., St. Louis, MO) 0.5 mM MgCl₂ and 1 mM EGTA.

Preparation of Brain Microtubules: Microtubule protein was purified from whole bovine brain by the procedure of Asnes and Wilson (7) as modified (8). After three cycles of purification by assembly/disassembly, the microtubule protein was stored at -80°C at concentrations of 17–23 mg/ml.

A MAP preparation of >90% MAP2 was obtained by heating the microtubule protein solution as described (9). The desalted solution was concentrated by ultrafiltration over a YM-30 Amicon filter (Amicon Corp., Danvers, MA).

Pellet Volume: In brief, microtubules were assembled in the presence of taxol, the solution was aliquoted into preweighed airfuge tubes, the microtubules were pelleted, the supernatant was removed, and the tubes were reweighed. Pellet volumes were then calculated assuming a specific gravity of 1.0. Pellets were solubilized and their protein was determined. We defined the microtubule specific volume as the pellet volume per unit of pellet protein expressed in microliters per milligram protein. Details of the protocol are as follows: freshly thawed three-times-cycled purified microtubule protein was assembled such that the final concentration before centrifugation was 10.65 mg/ml. Immediately after GTP-Mg was added to initiate assembly, taxol in dimethylsulfoxide was added to a final concentration of 154 μM taxol and 1% dimethylsulfoxide; incubation proceeded for 30 min at 30°. 170 μl of the solution was then distributed into each of three airfuge tubes (Beckman Ultra-Clear 5 × 20 mm; Beckman Instruments Inc., Fullerton, CA) and centrifuged in a Beckman Airfuge for 12.5 min at 10⁵ g. The rotor speed was approximated from the manufacturer's graph of speed versus pressure and verified by tachometer measurements (model 8205; Cole-Parmer Instrument Co., Chicago, IL). Supernatants were aspirated and the walls of the tubes were wiped dry with pointed swabs. The preweighed tubes were immediately reweighed and the pellets were solubilized in Lowry A solution. Protein was determined by the method of Lowry et al. (10) using bovine serum albumin as standard.

In experiments in which manipulations followed assembly, initial assembly volume was reduced to accommodate the addition of appropriate buffers or reagents. In all cases the final concentration of tubulin and the volume centrifuged remained constant.

Manipulation of Assembled Microtubules: Manipulations of pH and ionic strength were made possible by use of taxol stabilization. Vallee has shown that taxol allows the desorption of MAPs from microtubules by high salt without their depolymerization (11). In addition, we found that taxol also inhibits the disassembly of microtubules at alkaline pH. Most important, taxol also appears to prevent microtubule disassembly from the hydrostatic pressure well-known to develop during ultracentrifugation. Thus, consistent with the stabilization by taxol to cold (12), taxol microtubules centrifuged for prolonged periods were resistant to disassembly, whereas in the absence of taxol, disassembly was progressive with time of centrifugation. The pellets formed with or without taxol had the same specific volumes (±10–20%) and showed a similar pH-dependence. However, in the absence of taxol the pellet yield was small and variable, ranging from 10 to 80% of the taxol pellets (which varied <5%).

We used taxol in all experiments described. To manipulate pH, the solution of assembled microtubules in a 1.5-ml conical microfuge tube was first overlaid with 100–150 μl of the PG buffer described above. A predetermined amount of strong acid or base was then pipetted over the buffer to avoid direct contact with the microtubule suspension, and the entire contents was rapidly mixed by stirring with a fitted metal spatula. Incubation was continued for an additional 30 min.

An analogous procedure was followed for the addition of NaCl to a final concentration of 0.35 M. In this case, 3.75 M NaCl was carefully placed over the buffer layer and then mixed as for the pH shift experiments. The effective stabilization of microtubules by taxol was verified by the recovery of equal amounts of pellet tubulin in all cases (data not shown).

Chymotryptic Digestion: Assembled microtubule suspensions were

incubated with 1 μg/ml α-chymotrypsin (type 1-S; Sigma Chemical Co.) for 10 min, and the digestion was quenched with phenylmethane sulfonate in ethanol (1.5% ethanol) at a 2 mM final concentration (13). Pellet volumes were determined as described above. 1.5% ethanol alone had no effect on pellet volume.

MAP Supplementation: In these experiments, heat-stable MAPs—predominantly MAP2—were added before assembly in taxol.

Gel Electrophoresis Quantitation: Samples of pellets, supernatants, and other preparations were taken up in an equal volume of two-times-concentrated Laemmli sample buffer and electrophoresed through a 3.5% polyacrylamide stacking, 7.5% running gel in Tris-glycine-SDS (14). For quantitation, gels were stained in 0.25% Fast green FCF in 50% methanol, 10% acetic acid and destained in 7.5% acetic acid. The destained gel was scanned (Hoefer 6S 300 Transmittance scanning densitometer; Hoefer Scientific Instruments, San Francisco, CA) and the area under the peaks was quantified with a Graf-Pen sonic digitizer.

Viscometry: All conditions for assembly, pH adjustment, and other treatments were as described above except that the final protein concentration was 5 mg/ml. The falling-ball technique, as modified by MacLean-Fletcher and Pollard, was used (15). Capillaries used were 100-μl pipets (Corning Medical and Scientific, Medfield, MA); steel balls were 0.025 inches, grade 10 steel (N.E. Miniature Ball Co., Norfolk, CT). The capillaries were calibrated with glycerol-water solutions of known viscosity. Measurements were made at 30° in a stirred water bath. Ball velocity measurements were repeated three times over a 4-cm track that started 2 cm from the beginning of the ball descent.

Electron Microscopy: For thin-section analyses, the microtubules were pelleted by centrifugation under precisely the same conditions as for pellet volume determinations. After fixation in 1% glutaraldehyde the pellets were processed as previously described (16).

Microtubule density was determined from intersections on a line matrix placed over micrographs taken randomly over sections according to a table of random numbers (17). We counted only microtubules cut in cross-section to avoid ambiguities related to section thickness.

RESULTS

Standardization of Packed Microtubule Volume

We established standard conditions for centrifugation in which all sedimentable microtubules had been pelleted and the pellet specific volume approached a plateau. Fig. 1 shows the total pellet protein and specific volume (microliters of pellet per milligram of protein) as a function of the time of centrifugation at 10⁵ g. The total protein in the pellet reached a maximum at ~6–8 min. At the same time there was a leveling of the specific volume. Prolonged centrifugation for 60–120 min led to a gradual decrease in specific volume associated with a decrease in pellet protein that was probably due to pressure-induced microtubule disassembly (18). We adopted 12.5-min centrifugation time as standard. By this time, the pellet protein had reached a maximum with the complete sedimentation of formed microtubules. Although arbitrary, these fixed conditions allowed comparisons of re-

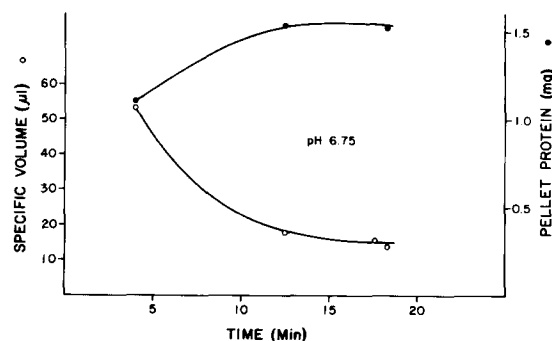


FIGURE 1 Effect of time of centrifugation on pellet protein and specific volume. The points are the average of triplicate samples drawn from the same assembled pool. Maximal sedimentation of protein and minimal specific volume were approached concurrently.

sults in which pH, ionic strength, or MAP content was varied. At pH 6.85, the mean specific volume was $22.4 \pm 4.3 \mu\text{l}/\text{mg}$ in 36 experiments.

Contribution of MAPs to Specific Volume

MAPs were removed from the taxol-stabilized microtubules either by addition of 0.35 M NaCl into the incubation mixture (11) or by limited digestion with chymotrypsin (13). As Vallee reported (11) for porcine microtubule protein, 0.35 M NaCl caused quantitative desorption of MAPs from bovine taxol-stabilized microtubules in our buffer system. Fig. 2a shows the electrophoretic pattern of pellet and supernatant proteins from solutions of taxol-stabilized microtubules incubated with

or without 0.35 M NaCl. The small amount of MAP present cannot be attributed to entrapped supernatant proteins (see below) and presumably represents the equilibrium binding of MAPs at this ionic strength. The mean specific volume after salt addition was $10.3 \mu\text{l}/\text{mg}$ protein (Table I).

Chymotryptic digestion of taxol-stabilized microtubules yielded a preparation in which the specific volume was $7.6 \mu\text{l}/\text{mg}$ protein, slightly less than that obtained by salt treatment. Under our experimental conditions, virtually all of the higher molecular weight MAPs (MAP1 and MAP2) were cleaved, leaving <2% MAPs as measured by densitometry. Thus, at least 70% of the packed volume of our four-times-cycled microtubule protein was determined by MAPs.

Effect of Increasing MAP2 on Specific Volume

Since the spacing between microtubules *in vivo* is variable, we sought to identify mechanisms that might regulate spacing *in vitro* as reflected by the specific volume of microtubule pellets. As noted, the spacing between microtubules is generally attributed to MAPs (12), but the quantitative relationship between MAP content and packing volume has not been defined. We found that increasing the MAP2 content of microtubules led to a proportional increase in packing volume.

The dramatic differences in specific volume obtained at different MAP concentrations is perhaps best appreciated from visual inspection of the microtubule pellets. Fig. 3 is a

TABLE I. Summary: Specific Volume of Microtubules

Treatment*	Specific volume (mean \pm SD) $\mu\text{l}/\text{mg}$ protein	n
Control	26.6 ± 4.1	11*
+0.35 M NaCl	10.3 ± 2.3	7
+Chymotrypsin	7.6 ± 0.8	4

n, number of experiments.

* As described in Materials and Methods, microtubules were assembled first, and NaCl or chymotrypsin was then added. The pellet tubulin as determined by Lowry and densitometry of SDS PAGE gels was constant.

* This average is of the 11 controls used in the NaCl and chymotrypsin experiments, and differs slightly from the 22.4 ± 4.3 figure for all 36 experiments.

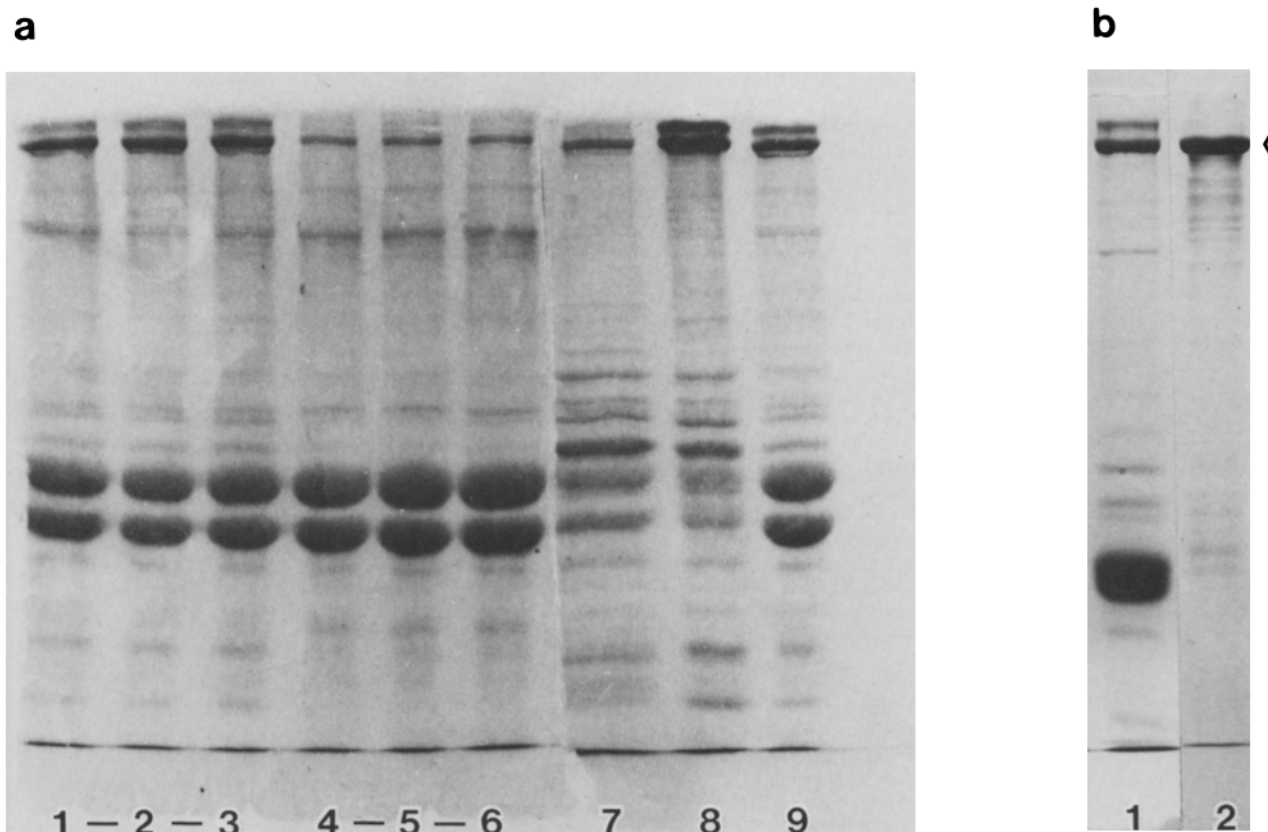


FIGURE 2 (a and b) Fast green-stained SDS PAGE. (a) Pellet and supernatant proteins in the presence or absence of 0.35 M NaCl ($80 \mu\text{g}$ protein/lane). Lanes: 1-3, pellet proteins of three identical samples without added salt; 4-6, pellet proteins of three identical salt-treated samples; 7, pooled supernatant of samples without added salt; 8, pooled supernatant of 0.35 M NaCl-treated samples; and 9, starting three-times-cycled microtubule protein. (b) MAP preparation used to enrich assembly mixture for MAPs ($80 \mu\text{g}$ protein/lane). Lane 1, three-times-cycled microtubule protein; lane 2, MAP preparation derived from material shown in lane 1. MAP 2 (arrowhead) accounted for $\sim 90\%$ of the total protein mass; tau proteins, for 2.5%.

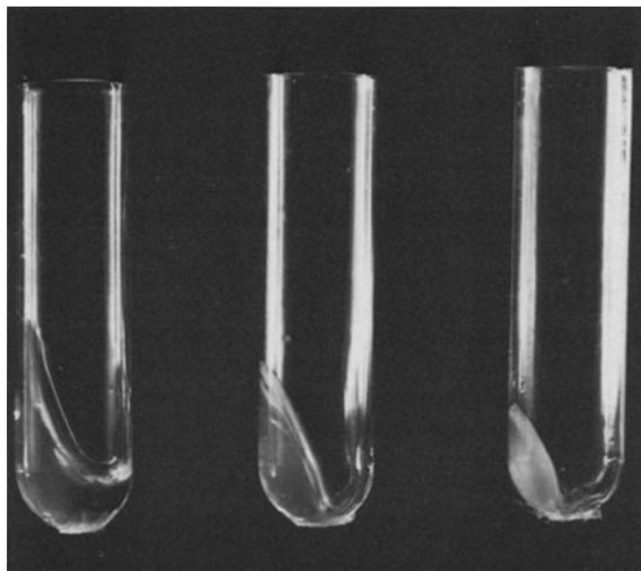


FIGURE 3 Photograph of microtubule pellets obtained at various MAP concentrations. The samples were centrifuged under standard conditions and the supernatants were removed. Subsequent measurements of the specific volumes from the pellets in the photographs gave values (from left to right) of 48.9, 23.9, and 7.8 $\mu\text{l}/\text{mg}$ protein. Densitometry of the pellets after SDS PAGE gave MAP contents of 30, 23, and 2%, respectively.

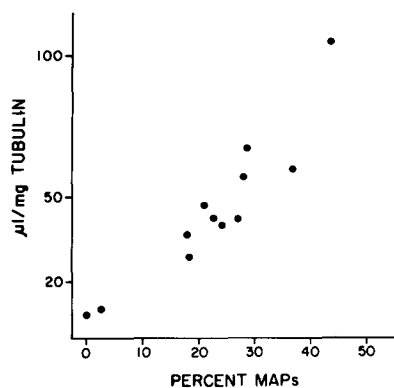


FIGURE 4 Effect of MAP content on pellet specific volume. Specific volume is expressed as microliters per milligram tubulin to emphasize the volume contributed by MAPs to a fixed quantity of microtubules. MAPs were added before assembly. MAP pellet content was determined by densitometry of SDS PAGE gels stained with Fast green and is expressed as percentage of total protein mass.

photograph of pellets after centrifugation and removal of the supernatant. From left to right the pellet MAP content was 30% (MAP added to four-times-cycled microtubule protein), 23% (four-times-cycled microtubule protein) and 2% (four-times-cycled microtubule protein plus 0.35 M NaCl). The corresponding specific volumes were 48.9, 23.9, and 7.8 $\mu\text{l}/\text{mg}$ protein, respectively. In additional studies we systematically varied MAP content.

We prepared crude MAP2 (heat-stable MAPs) which was then added in increasing amounts to the microtubule protein assembly mixture. Fig. 2b shows a Fast green-stained gel of the MAP preparation used in these experiments. By scanning densitometry of the gel, MAP2 accounted for >90% of the protein. After assembly, specific volume was determined in the usual way. The MAP content of the pellet protein was

determined by densitometry. Fig. 4 shows the relationship between specific volume and HMW MAP content expressed as percentage of the total protein mass. The graph shows an approximately linear relationship between MAP content and the specific volume expressed as microliters per milligram of tubulin, varying from 7.6 to 105, roughly 14-fold. At the highest MAP content studied, the molar ratio of MAP2 to tubulin was 0.32.

In general, we have assumed that the MAP content of pellets is microtubule bound. Neither salt-desorbed MAPs nor the heat-stable MAP preparation was sedimentable under the conditions of our experiments. To determine more rigorously whether all of the pellet MAP was bound to microtubules or whether there was significant free MAP, we centrifuged the assembled mixture through a sucrose-taxol cushion (11) and compared the pellet MAP content to that of an unwashed pellet. No difference was found in the MAP content (Table II). Therefore, we can conclude that there was little free MAP in the pellet.

The presence of MAPs per se (without attachment to microtubules) did not affect specific volume. Thus, when 0.35 M NaCl was added to strip-bound MAPs before sedimentation, the specific volumes obtained subsequently were identical irrespective of the MAP concentration used during microtubule assembly.

Effect of pH on Specific Volume

We showed previously that pH has profound effects on microtubule assembly in vitro without altering MAP content (8) and that microtubule disassembly is associated with an increase in cytosolic pH (19). In search of physiologic regulators of microtubule spacing, we examined the effects of pH on the specific volume of pellets. Taxol-stabilized microtubules were assembled first, and the pH of the suspension was then adjusted as described in Materials and Methods. In this way, the effects of pH on microtubule assembly and length distribution per se (8) did not affect the specific volume. Fig. 5, a and b, show that the pelleting was complete and the specific volume was approximately constant under the standard conditions of centrifugation. Fig. 6 shows that the specific volume increased linearly with pH, roughly doubling over the range of pH from 6.0 to 7.5. Since specific volume was shown above to be related to MAP content, it seemed possible that the observed volume changes were only indirectly dependent on pH, which might have affected the association of MAPs with microtubules. We showed previously, however, that the MAP content of microtubules assembled in the absence of taxol was unaffected by pH (8). Quantitation of taxol-stabi-

TABLE II. MAP Content of Microtubule Pellets Collected by Centrifugation With or Without Sucrose Cushion

Experiment	Preparation*	% HMW-MAPs	
		Without cushion	With cushion
1	A	13.0	14.1
2	A + MAP*	21.3	21.7
3	A + MAP	17.3	20.3
4	B	21.7	23.0

* A and B were two separate preparations of bovine microtubule protein.

† In experiments 2 and 3, supplementary MAP2 was added before assembly as in the experiments of Figs. 3 and 4.

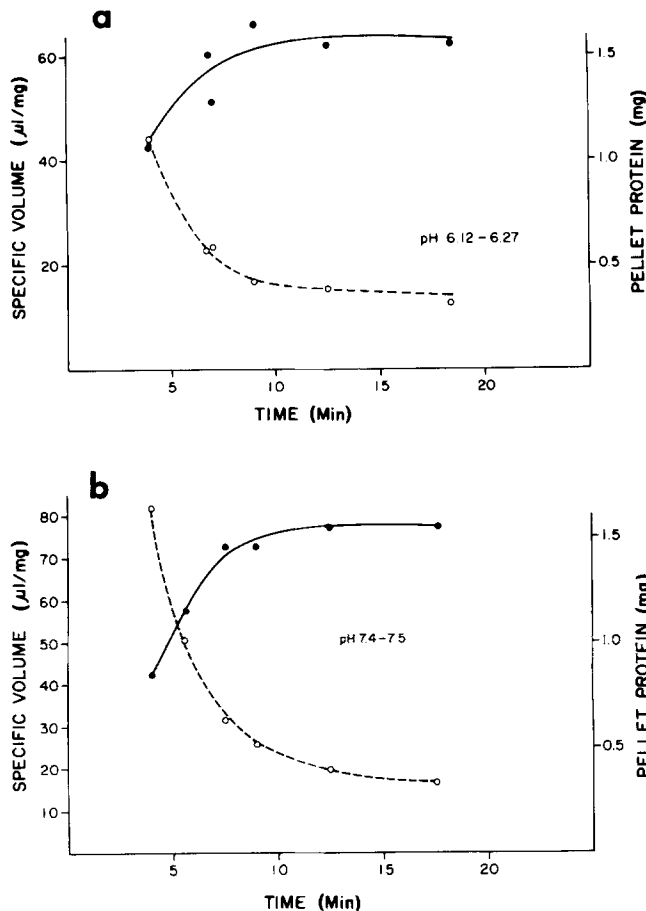


FIGURE 5 (a and b) Effect of time of centrifugation on pellet total protein and specific volume at acid and alkaline pHs. The procedure was as for Fig. 1. (a) pH 6.12-6.27 (range of triplicates). (b) pH 7.4-7.5 (range of triplicates).

lized pellet proteins showed that the MAP content of these microtubules was also independent of pH. The percentage of total protein mass, expressed as HMW-MAPs (1 and 2) relative to the total mass determined by densitometry of Fast green-stained SDS PAGE gels of pellet proteins, was as follows: 17.5 at pH 5.5, 15.5 at pH 6.3, 20 at pH 6.8, and 18.7 at pH 7.4. Thus, low pH was functionally equivalent to removing MAPs.

The specific volume of microtubules depleted of MAPs by incubation in 0.35 M salt or by chymotryptic digestion was independent of pH (data not shown). Consequently, although pH did not exert its effect by altering MAP content, the pH effect on specific volume was nevertheless dependent on MAPs.

Electron Microscopy of Thin Sections through Microtubule Pellets

Fig. 7, a and b, shows representative sections from pellets obtained from microtubule suspensions at pH 6.0 and 7.4, respectively. The higher packing density at low pH is obvious to the eye. Point counting of microtubules per unit area gave approximately double ($\times 1.75$) microtubule density at pH 6.0 as at pH 7.4. In the experiment illustrated, replicate pellets processed for direct volume determinations showed a somewhat lesser pH effect than usual: 18.6 and 30.5 $\mu\text{l}/\text{mg}$ protein at the low and high pH respectively. This difference of 1.64-

fold is remarkably close to the change in microtubule density determined by morphometry.

Viscosity of Taxol-stabilized Microtubules

One possible physical structure that could account for the high specific volume of microtubule pellets is a cross-linked hydrated gel. Characteristic of such gels is an elevated solution viscosity (15). We found, however, using both falling-ball and Ostwald viscometers, that the viscosities of suspension of taxol-stabilized microtubules were only in the range of 20-300 centipoise (Fig. 8). Moreover, the viscosity declined with pH, whereas we showed above that increasing pH increased specific volume. Thus, there was no evidence of significant cross-linking between microtubules.

DISCUSSION

The packing volume of microtubules (or other structures) will be a function of their size, shape, and the force applied to them. We standardized the centrifugation procedure to reduce differences due to mechanical forces. Specifically, measurements were taken after the pellet protein content became constant and the pellet specific volume decreased $<10\%$ with a doubling of centrifugation time. Under our conditions the mean specific volume of the pellets was 22 $\mu\text{l}/\text{mg}$ protein for microtubules assembled from three-times-cycled bovine brain microtubule protein. Solutions of collagen mixed with purified GAGs have been centrifuged under similar conditions and the water content of the pellets obtained is of the same magnitude. For example, when hyaluronate with collagen is pelleted at $10^5 g$ for 30 min, its specific volume is found to be 10-40 $\mu\text{l}/\text{mg}$ (20). This property of GAGs has been associated with their capacity to create a fluid, incompressible extracellular matrix (3). The similarity of the specific volumes of GAGs and microtubules indicates that they resist compression equally. Thus, microtubules could function as an intracellular matrix whose mechanical properties would be highly similar to the extracellular matrix formed by GAGs.

Quantitative analysis of the packing volume described has important implications for the contribution of microtubules to the organization of cytoplasmic space. To apply our results, we first consider the orientation of microtubules in pellets as compared with cells since orientation will affect packing density. The generally parallel microtubule arrays in axons,

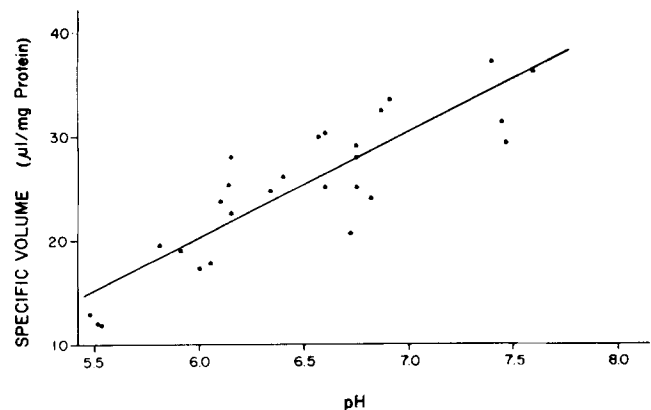


FIGURE 6 Effect of pH on specific volume. pH was adjusted after assembly. Each point is an average of triplicates. The line is a least squares fit: $y = 10.2; x = 41.0; r^2 = 0.76$.

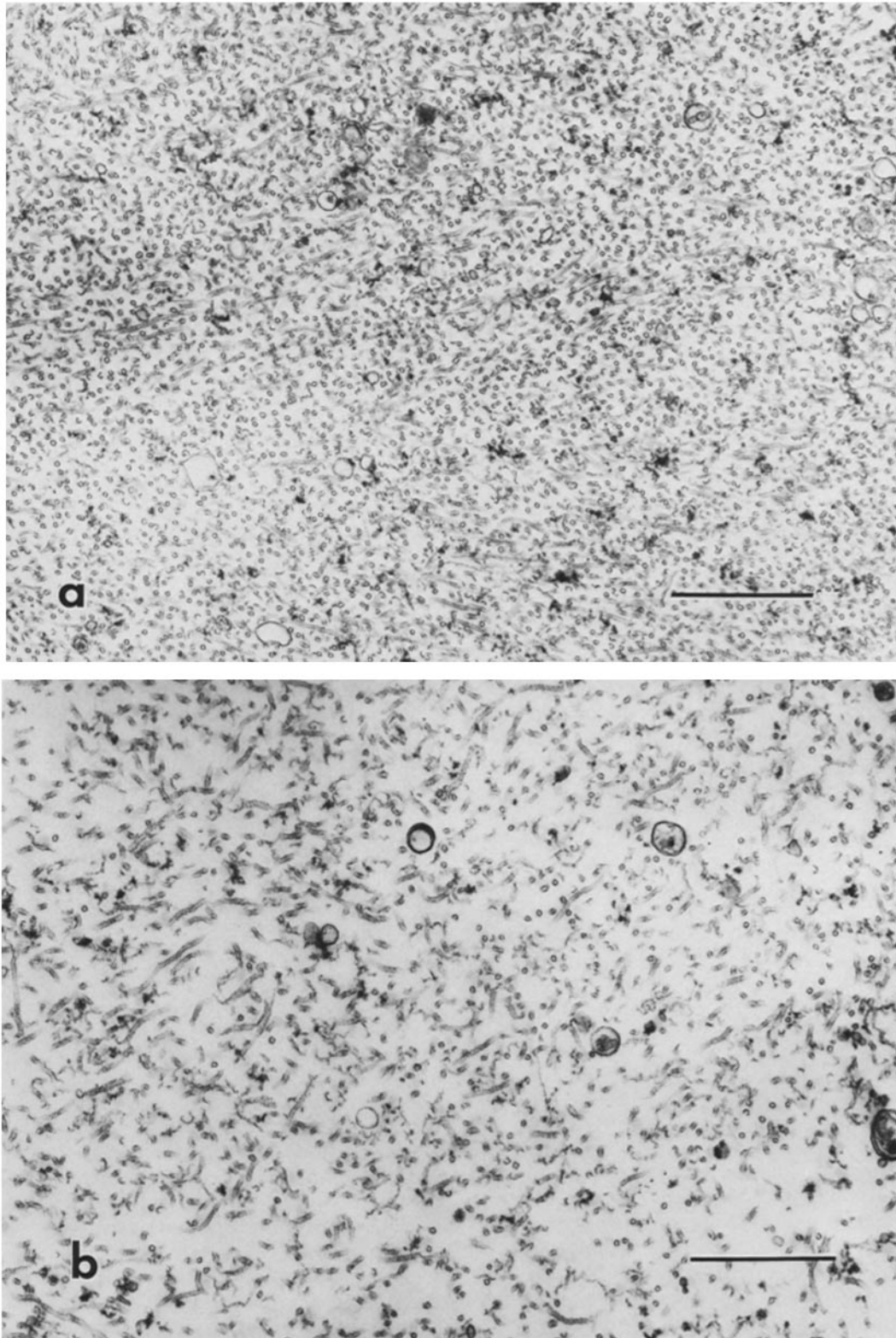


FIGURE 7 (a and b) Microtubule pellets at pH 6.0 and 7.4. After assembly at pH 6.75 microtubule suspensions were shifted to pH 6.0 or 7.4 and pelleted as described in Materials and Methods. (a) pH 6.0. (b) pH 7.4. Bar, 1.0 μm . $\times 22,000$.

for example, may approach optimum packing (least empty space), which is a hexagonal array for straight cylinders (21). It might be anticipated that microtubule orientation in pellets would be random as compared with the roughly parallel microtubule arrays observed *in vivo*. However, thin sections

through pellets usually show large areas in which microtubules are parallel (reference 2 and Fig. 6), and theoretical analysis given below indicates that predominantly parallel arrays are to be expected. We believe microtubule orientation in pellets may be understood in terms of the behavior of liquid crystals

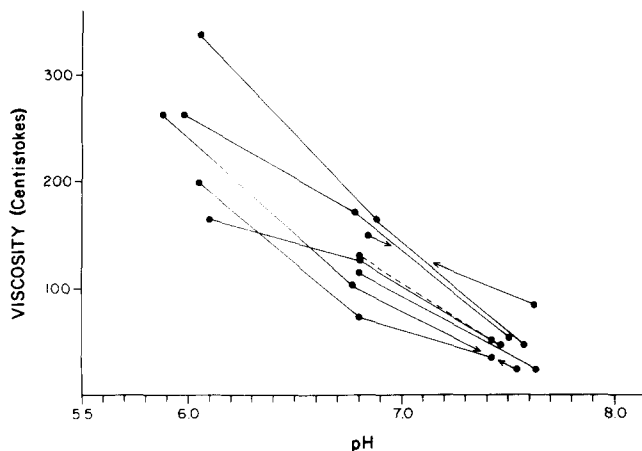


FIGURE 8 Viscosity of microtubule suspensions as a function of pH. The viscosities of microtubule suspensions at a concentration of 5 mg/ml were measured at 30° by the falling ball method and confirmed in Ostwald viscometers at selected points (data not shown).

approaching a phase transition (the isotropic–nematic liquid–crystal phase transition) (22). Note that an essential requirement for liquid crystalline behavior is a population of highly anisotropic noninteracting molecules (22), and that since Onsager’s initial formulation (23), theoretical treatments of liquid crystals have been based on considerations of a fluid of long hard rods. More recently, the theory and experiment have been brought into closer agreement by allowing for semiflexible rods (24). Obviously, microtubules are highly anisotropic and semirigid (25), and our viscosity measurements show them to be essentially noninteracting.

As a solution of rod-shaped molecules is concentrated, there is a transition from a random orientation to one of increasing local order, which takes the form of their parallel orientation. It can be predicted that for rods with an axial ratio $l/d > 10$, a nematic phase transition will occur when $c > 5/dl^2$, where l is the rod length, d is the rod diameter, and c is the number of rods per unit volume (26). In a microtubule pellet wherein the specific volume is 22 $\mu\text{l}/\text{mg}$ protein, c is $1.01 \times 10^{14}/\text{cm}^3$, and $5/dl^2 = 0.74 \times 10^{14}/\text{cm}^3$ (see Appendix A); thus, nematic phase transition during pelleting is to be expected. In a recent theoretical paper (26), Edwards and Evans indicate that in concentrated solutions the translational diffusion constant of the rods, D , effectively goes to zero. In effect, the microtubule pellets form a glass. The mechanical stabilities of microtubule pellets are consistent with this interpretation. Thus, the pellets at specific volumes of 8 and 24 $\mu\text{l}/\text{mg}$ protein retain their shape for long periods (Fig. 3). With high MAP content and specific volume the lower rod concentration allows the pellet to “relax.” The parallel orientation of microtubules that can be predicted from a nematic phase transition suggests that microtubule packing is far from random and may be similar to the characteristically parallel orientation of microtubules in cells. Moreover, direct calculation shows that the degree of packing in pellets is within two- or threefold of optimum (minimum space occupancy). Taking the microtubule radius as 15 nm and 1,625 tubulin dimer subunits per μm length, we can calculate that 1 mg of microtubules (without MAPs) occupies a volume of 2.5 μl . Even if the microtubules were optimally packed rods in which 90% of space is occupied (21), the packed volume would be $\sim 2.9 \mu\text{l}/\text{mg}$ protein. When

assembled microtubules were stripped of MAPs by chymotrypsin, the mean specific volume of pellets was 7.6 $\mu\text{l}/\text{mg}$ protein (Table I), only some 2.5 times the optimal.

Since microtubules in cells are often not in precise hexagonal arrays (i.e., they are packed suboptimally), we can assume that pellet specific volumes at least approach the physiological condition. Given this, the measured pellet specific volumes suggest that a large fraction of the volume of cytosol is occupied by microtubules. For example, Schliwa and Eute-neuer estimate by morphometry that the concentration of assembled tubulin in the cytoplasm of fish erythrocytes is 16.5 mg/ml (27). At an approximate intracellular pH of 7.0 and with a MAP content similar to that present in our bovine brain preparations, this would correspond to a pellet volume of $\sim 400 \mu\text{l}/\text{ml}$, i.e., 40% of the volume of cytosol. Of course, the nature of erythrocyte MAPs is unknown. Perhaps better examples are to be found in nervous tissue. In axons, our calculations from published photomicrographs (5) indicate that in some instances the microtubules alone (without MAPs) account for $>50\%$ of the cross-sectional area. If MAPs are assumed to be present, the regularity of microtubule distribution suggests that the approach of neighboring axonal microtubules may be limited and that their packing approximates that of microtubules in pellets. Since the latter is obtained at very high g forces, we suggest that the spread arrays of microtubules seen in structures such as axons constitute a mechanically irreducible volume.

In other physiological situations, microtubules are not widely separated. For example, in the initial segment of neurons, microtubules are found characteristically in bundles in which the walls of microtubules often appear to touch (6). This arrangement, we find, cannot be achieved at high g forces with microtubules that contain a normal complement of MAPs and/or neutral pH. Consequently, it is possible that the local approximation of microtubules occurs with corresponding changes in pH and/or MAP content (or other factors yet unidentified). Similarly, we suspect that microtubules in regions of the spindle, midbody, or near centrioles may have specifically altered MAP content or pH environments. We should emphasize that the pH effects occur at constant MAP content. Elevating pH may cause the HMW-MAP side-arm to become more extended or more perpendicular to the microtubule wall, and the conformation of these proteins as a function of pH warrants investigation.

Of other biological structures probably skeletal muscle has been treated most extensively as a liquid crystal (reviewed in reference 28). The parallel orientation of myosin fibers has been described in terms of a smectic liquid crystalline array (clearly more ordered than the nematic forms we have discussed, which condense from relatively dilute solutions). It is interesting that in muscle, interfilament distance also decreases with pH (albeit relatively little above pH 6); this has been attributed to reduction of surface molecular charge (29). The molecular organization of muscle makes it possible to examine the effects of high ionic strength, whereas the microtubule-MAP structure is dissociated at high ionic strengths. However, the effects of increasing osmolarity on muscle and centrifugation on microtubule pellets are analogous, and in both cases, increases lead to decrease in packed volume which asymptotically becomes nearly constant.

If microtubules may indeed be irreducibly packed in certain regions of the cell, what limitations are placed on molecular or particle movement between them? Our analysis applies to

free entities, unbound to microtubules or MAPs. The general problem of transport or penetration of particles through polymers has been considered by Ogston (30), who showed that the partition coefficient (ratio of concentration in polymer gel to that in free solution), K , is equal to $\exp[-\pi L(r_s + r_f)^2]$, where L is the fibril length per unit volume and r_s and r_f are the radii of particle and fiber, respectively. To apply this theory to arrays of microtubules (Appendix B), we consider two extreme cases: case 1, MAP-free pellets with specific volumes of 7.6 $\mu\text{l}/\text{mg}$ protein, and case 2, microtubule pellets at alkaline pH or with additional MAPs with specific volumes of 40 $\mu\text{l}/\text{mg}$ protein. For $K = 0.1$, and thus for the diffusion coefficient to be reduced by $\sim 90\%$, it is readily calculated for the MAP-free pellet (case 1) that particle size must be ~ 25 nm, nearly twice the radius of the microtubule itself. For the MAP-containing pellet (case 2), we considered the contribution of MAPs in two ways: (a) that MAPs simply increase the effective radius of the microtubule from 15 to 35 nm (roughly the full length of the MAP2 sidearm ([31]), or (b) that the MAPs themselves constitute the relevant fiber network. In either case, only the movement of large particles, ~ 25 nm in radius, would be affected. Thus, networks of uncross-linked microtubules would not be expected to impede diffusion of proteins in solution but would block the movement of even small vesicles. This prediction is in general accord with measurements of molecular diffusion by either electron spin resonance (32) or fluorescence (33) techniques: the translational diffusion coefficient for small molecules is within two- or threefold of that in aqueous solution. Retardation of some proteins could be attributed to transient binding on the cytomatrix. On the other hand, treatment of cells with hypertonic solutions to extract water and presumably condense the cytomatrix slows translational movement appreciably (33). We would suggest from our analysis that this reduction in diffusion cannot result from movement through a microtubule array. Rather, a finer-grained network would be required, perhaps cross-linked to microtubules. This network would have to be intercalated between microtubules in order to increase the effective fiber radius in the Ogston equation. The microtrabecular lattice has been depicted in precisely such an arrangement (34). It is thus not surprising that diffusion in the cytosol, examined as a whole, would not be affected by the cytomatrix. More specialized regions or cells, however, might contain a sufficiently dense cytomatrix to affect diffusion. A functional test of the presence of such a lattice, for example, would be the measurement of macromolecular diffusion in erythrocytes whose cytoplasm has been described in terms of an intertwined lattice of microtubules and microtrabeculae.

GAG-collagen gels and microtubules, while occupying similar volumes, would have different effects on diffusion. GAGs significantly impede translational diffusion (3, 4). We predict (above) that microtubules would not. This paradox is explainable in terms of the Ogston equation. The length of fiber per unit volume, L , per unit mass, is much longer for GAGs composed of a single chain than for the 13-stranded microtubule. Teleologically it seems appropriate that an intracellular matrix of microtubules could provide the cell or its processes with a mechanically stable minimum volume that yet allowed free movement of macromolecules within that volume; comparable movement within a stable extracellular matrix may not be necessary.

We recognize that extrapolation from pelleted microtubules to the physiological situation is difficult. However, our study shows that partially oriented microtubules may form a liquid crystal that occupies considerable volume even when packed at high g forces. The surprising size of its specific volume and the high concentrations of tubulin in certain cells and/or their processes suggest that microtubules are a major determinant of cell volume as well as cell shape. Indeed, microtubule disassembly causes a volume decrease (35). Microtubules may form a highly permeable matrix that allows the free diffusion of proteins but may impede vesicular traffic. For this reason alone, vesicular transport may take place via special mechanisms. The microtubule matrix may also accommodate other fibrous elements or microtrabeculae which then become determinants of diffusion processes. Finally, we have shown that the space occupied by microtubules is highly dependent on pH and MAP content, suggesting ways in which the properties of the microtubule matrix may be modified. Out of this undoubtedly complex intracellular matrix, our analysis has sought to define more precisely the potential contribution of microtubules per se to structural stability, volume, and the diffusion/movement of macromolecules within cells.

Appendix A

Following are evaluations of c , number of rods per unit volume, and of $5/dl^2$, where d is rod diameter and l is rod length.

22 $\mu\text{l}/\text{mg}$ tubulin is 45 mg tubulin/ml. With 1.625 dimers/ μm microtubule length, a mean length of taxol-stabilized microtubules of 1.5 μm (12), and a dimer molecular weight of 110,000,

$$c = \frac{45 \text{ mg/ml}}{1.1 \times 10^5 \text{ mg/mmol}} \times \frac{6.023 \times 10^{20} \text{ molecules/mmol}}{1.625 \times 10^7 \text{ molecules/cm microtubule} \times 1.5 \times 10^{-4} \text{ cm (average length of taxol microtubule)}} = 1.01 \times 10^{14} \text{ microtubules (rods)/cm}^3.$$

Taking d as 30 nm,

$$5/dl^2 = \frac{5}{(3.0 \times 10^{-6} \text{ cm}) \times (1.5 \times 10^{-4} \text{ cm})^2} = 0.74 \times 10^{14}.$$

Appendix B

Following is an evaluation of the partition coefficient K of a particle into a fiber network.

$$K = \exp[-\pi L(r_s + r_f)^2],$$

where L is the fiber length per unit volume (centimeters per milliliter) and r_s and r_f (centimeters) are the radii of particle and fiber, respectively.

L' is defined as L per milligram protein.

$$L' = \frac{1 \text{ mg}}{1.1 \times 10^5 \text{ mg tubulin/mmol}} \times \frac{6.023 \times 10^{20} \text{ molecules/mmol}}{1.625 \times 10^7 \text{ molecules tubulin/cm microtubule}} = 3.37 \times 10^8 \text{ cm microtubule/mg protein.}$$

$$L = L' \times c.$$

Case 1

For this case, the parameters are no MAPs; $r_f = 15$ nm; and $c = 1/7.6 \mu\text{l}$ per mg or 132 mg/ml.

$$\ln K = -1.059 \times 10^9 \text{ cm} \times 132 \text{ mg/ml} \times (r_s + 1.5 \times 10^{-6} \text{ cm})^2.$$

For $K = 0.1$, $r_s = 26$ nm.

Case 2

For this case, $r_t = 35$ nm; and $c = 25$ mg/ml. We consider two possibilities:
(a) MAPs simply increase the effective r_t .

$$\ln K = -1.059 \times 10^9 \times 25 \times (r_s + 3.5 \times 10^{-6} \text{ cm})^2.$$

Again, for $K = 0.1$, $r_s = 58$ nm.

(b) MAPs are the true fibrous network. L (length of fiber per unit volume) is now increased by the combined length of the MAP side-arms. For a MAP/tubulin ratio of 0.32 there are ~ 500 (1625×0.32) MAPs/ μm of microtubule. If each side arm is assumed to be 20 nm, the combined length of MAP per micrometer of microtubule is 500×20 nm, or $10 \mu\text{m}$. Thus, the total length of MAPs is 10-fold that of the microtubule itself, calculated above to be 3.37×10^8 cm/mg per ml, i.e., $L' = 3.37 \times 10^9$ cm/mg per ml. Assuming the MAP radius to be 4 nm and taking $c = 1/40 \mu\text{l}/\text{mg} = 25$ mg/ml,

$$\ln K = -1.059 \times 10^{10} \times (r_s + 0.4 \times 10^{-6} \text{ cm})^2 \times 25.$$

For $K = 0.1$, $r_s = 25$ nm.

This work was supported by grant CA 15544 from the National Institutes of Health.

Received for publication 9 April 1984, and in revised form 6 May 1985.

REFERENCES

- Porter, K. R. 1966. Cytoplasmic microtubules and their functions. *Ciba Found. Symp. Principles Biomol. Organ.* 12:308-345.
- Kim, H., L. I. Binder, and J. L. Rosenbaum. 1979. The periodic association of MAP2 with brain microtubules in vitro. *J. Cell Biol.* 80:266-276.
- Comper, W. D., and T. C. Laurent. 1978. Physiological function of connective tissue polysaccharides. *Physiol. Rev.* 58:255-315.
- Meyer, F. A. 1983. Macromolecular basis of globular protein exclusion and of swelling pressure in loose connective tissue (umbilical cord). *Biochim. Biophys. Acta.* 755:388-399.
- Bray, D., and M. B. Bunge. 1981. Serial analysis of microtubules in cultured rat sensory axons. *J. Neurocytol.* 10:589-605.
- Peters, A., S. L. Palay, and H. deF. Webster. 1976. *The Fine Structure of the Nervous System.* W.B. Saunders Co., Philadelphia. 406 pp.
- Asnes, C. F., and L. Wilson. 1979. Isolation of bovine brain microtubule protein without glycerol: polymerization kinetics change during purification cycles. *Anal. Biochem.* 98:64-73.
- Regula, C. S., J. R. Pfeiffer, and R. D. Berlin. 1981. Microtubule assembly and disassembly at alkaline pH. *J. Cell Biol.* 89:45-53.
- Fellous, A., J. Francon, A. M. Lennon, and J. Nunez. 1977. Microtubule assembly in vitro: purification of assembly-promoting factors. *Eur. J. Biochem.* 78:167-174.
- Lowry, O. H., N. J. Rosebrough, A. L. Farr, and R. J. Randall. 1951. Protein measurement with the Folin phenol reagent. *J. Biol. Chem.* 193:265-275.
- Vallee, R. B. 1982. A taxol-dependent procedure for the isolation of microtubules or MAPs. *J. Cell Biol.* 92: 435-442.
- Schiff, P. B., J. Fant, and S. B. Horwitz. 1979. Promotion of microtubule assembly in vitro by taxol. *Nature (Lond.)* 277:665-667.
- Vallee, R. B. 1980. Structure and phosphorylation of MAP2. *Proc. Natl. Acad. Sci. USA.* 77:3206-3210.
- Laemmli, U. K. 1970. Cleavage of structural proteins during the assembly of the head of bacteriophage T4. *Nature (Lond.)* 227:680-685.
- MacLean-Fletcher, S., and T. D. Pollard. 1980. Viscometric analysis of the gelation of *Acanthamoeba* extracts and purification of two gelation factors. *J. Cell Biol.* 85:414-428.
- Berlin, R. D., and J. M. Oliver. 1978. Analogous ultrastructure and surface properties during capping and phagocytosis in leukocytes. *J. Cell Biol.* 77:789-804.
- Weibel, E. R. 1979. *Stereological Methods. Vol. 1. Practical Methods for Biological Morphometry.* Academic Press, Inc., New York. 425 pp.
- Salmon, E. D. 1975. Pressure-induced depolymerization of brain microtubules in vitro. *Science (Wash. DC)* 189:884-886.
- Huntley, R., J. M. Oliver, and R. D. Berlin. 1981. Microtubule disassembly in vivo by colchicine is an autocatalytic process that depends on an induced intracellular alkalization. *J. Cell Biol.* 91(No. 2, Pt. 2):134a. (Abstr.)
- Disalvo, J., and M. Schubert. 1966. Interaction during fibril formation of soluble collagen with cartilage proteinpolysaccharide. *Biopolymers.* 4:247-258.
- Rogers, C. A. 1964. *Packing and Covering.* Cambridge University Press, Cambridge. 111 pp.
- Chandrasekhar, S. 1977. *Liquid Crystals.* Cambridge University Press, Cambridge. 148 pp.
- Onsager, L. 1949. The effects of shape on the interaction of colloidal particles. *Ann. NY Acad. Sci.* 51:627-659.
- Wulf, A., and A. G. DeRocco. 1971. Statistical mechanics for long semiflexible molecules: a model for the nematic mesophase. *J. Chem. Phys.* 55:12-27.
- Yamazaki, S., T. Maeda, and T. Miki-Nomura. 1982. Flexural rigidity of singlet microtubules estimated from statistical analysis of fluctuating images. In *Biological Functions of Microtubules and Related Structures.* H. Sakai, H. Mohri, and G. G. Borisy, editors. Academic Press Japan Inc., Tokyo. 453.
- Edwards, S. F., and K. E. Evans. 1982. Dynamics of highly entangled rod-like molecules. *J. Chem. Soc., Faraday Trans. II.* 78:113-121.
- Schliwa, M., and U. Euteneuer. 1978. Quantitative analysis of the microtubule system in isolated fish melanophores. *J. Supramol. Struct.* 8:177-190.
- Hawkins, R. J., and E. W. April. 1983. Liquid crystals in living tissues. *Adv. Liq. Cryst.* 6:243-264.
- April, E. W., P. W. Brandt, and G. F. Elliott. 1972. The myofilament lattice: studies on isolated fibers. II. The effects of osmotic strength, ionic concentration, and pH upon the unit-cell volume. *J. Cell Biol.* 53:53-65.
- Ogston, A. G., B. N. Preston, and J. D. Wells. 1973. On the transport of compact particles solutions of chain polymer. *Proc. R. Soc. Lond. A.* 333:297-316.
- Murphy, D. B., and G. G. Borisy. 1975. Association of high-molecular weight proteins with microtubules and their role in microtubule assembly in vitro. *Proc. Natl. Acad. Sci. USA.* 72:2696-2700.
- Mastro, A. M., M. A. Babich, W. D. Taylor, and A. D. Keith. 1984. Diffusion of a small molecule in the cytoplasm of mammalian cells. *Proc. Natl. Acad. Sci. USA.* 81:3414-3418.
- Jacobson, K., and J. Wojcieszyn. 1984. The translational mobility of substances within the cytoplasmic matrix. *Proc. Natl. Acad. Sci. USA.* 81:6747-6751.
- Wolosewick, J. J., and K. R. Porter. 1979. Microtubular lattice of the cytoplasmic ground substance: artifact or reality? *J. Cell Biol.* 82:114-139.
- Melmed, R. N., P. J. Karanian, and R. D. Berlin. 1981. Control of cell volume in the J774 macrophage by microtubule disassembly and cyclic AMP. *J. Cell Biol.* 90:761-768.